

Investigation of Umbral Dots with the New Vacuum Solar Telescope

Kaifan Ji¹ · Xia Jiang^{1,2} · Song Feng^{1,2} ·
Yunfei Yang^{1,2} · Hui Deng¹ · Feng Wang¹ ·

© Springer ●●●

Abstract

Umbral dots (UDs) are small isolated brightening observed in sunspot umbrae. They are convective phenomena existing inside umbrae. UD are usually divided into central UD (CUDs) and peripheral UD (PUDs) with respect to their positions inside an umbra. Our purpose is to investigate UD properties and analyze their relationships, and further to find whether or not the properties depend on the umbral magnetic field variation. For the purpose, we selected the high-resolution TiO images of four active regions (ARs) obtained under the best seeing conditions with the *New Vacuum Solar Telescope* (NVST) in Fuxian Solar Observatory of Yunnan Astronomical Observatory, China. The four ARs (NOAA 11598, 11801, 12158, and 12178) include six sunspots. A total of 1220 CUDs were extracted from six sunspots, and 603 PUDs from three sunspots. Meanwhile, the radial component of the magnetic field of the sunspots obtained with the *Helioseismic and Magnetic Imager* onboard the *Solar Dynamics Observatory* was used to analyze the influence to UD properties. To CUDs, their diameters and lifetimes exhibit an increasing trend with brightness, whereas their horizontal velocities exhibit an inverse trend. Moreover, the properties: diameter, intensity and velocity depend on magnetic field variation. To a CUD, its diameter becomes larger and brighter, and its motion shows slower in a weak magnetic field than in a strong field. To PUDs, the similar trends are also found. Moreover, we also find that the lifetimes of UD located in different sunspots are not obviously different, implying that they are unrelated to the magnetic flux density in which they lived.

Keywords: Sunspots, Umbra; Sunspots, Magnetic Fields

¹ Faculty of Information Engineering and Automation /
Yunnan Key Laboratory of Computer Technology
Application, Kunming University of Science and Technology,
Kunming 650500, China email: ynkmsf@escience.cn

² Key Laboratory of Solar Activity, National Astronomical
Observatories, Chinese Academy of Sciences, Beijing
100012, China

1. Introduction

There are some small bright features called umbral dots (UDs) in a dark umbra, and the features can be found almost all over umbrae and pores. UD only cover 3–10 % umbral area, but contribute 10–20 % brightness (Sobotka, Bonet, and Vazquez, 1993). This implies that convective motions must exist within umbrae because radiation cannot explain the phenomena. Therefore, UD play a vital role in the energy balance of sunspots. The study of UD is crucial to understanding the convective motions and the interactions of plasma with strong magnetic fields, and analyzing the formation mechanism of sunspots. Usually, UD are generally divided into two classes according to their origins (Grossmann-Doerth, Schmidt, and Schroeter, 1986). The UD are called peripheral UD (PUDs) near the penumbra-umbra boundary and central UD (CUDs) in the umbral center region. PUDs are generally brighter than CUDs, and quickly move toward the center of the umbra, however, CUDs are relatively static. Two different models have been proposed to explain the formation mechanism of UD: clustered magnetic flux tube and monolithic flux tube model. The former considers that UD are a hot field-free gas intruded into a cluster of magnetic flux tubes (Parker, 1979). The latter suggests that the energy transports in an umbra are dominated by non-stationary narrow plumes of rising hot plasma with adjacent downflows. The UD are formed by the narrow upflow plumes that become almost field-free near the surface layer (Schüssler and Vögler, 2006). The essential difference between the two models is that at the boundary UD exist the local downflows in the monolithic flux tube model. Detail studies of the physical properties of UD, such as morphology, velocity, lifetime, and intensity, and their relationships between different properties are crucial to understanding the nature of the local convective motions (Sobotka, Brandt, and Simon, 1997a,b; Bharti, Joshi, and Jaaffrey, 2007; Riethmüller *et al.*, 2008; Watanabe *et al.*, 2012).

Our aim is to analyze the properties of UD, and the relationships between different properties, and further to find whether or not the properties depend on the umbral magnetic field variation. So we select the high-resolution observations of four active regions (ARs) obtained under the best seeing conditions with the New Vacuum Solar Telescope (NVST) in Fuxian Solar Observatory of Yunnan Astronomical Observatory, China. The four ARs include six sunspots.

The layout of the paper is as follows: The observations and data reduction are described in Section 2. Section 3 briefly describes the identification procedure of CUDs and PUDs. Section 4 illustrates the physical properties of CUDs and PUDs, and their relationships between different properties. Moreover, the relationship and the influence to the properties with respect to different magnetic field are discussed. Finally, we give our conclusions in Section 5.

2. Observations and Data Reductions

The NVST is a vacuum solar telescope with a 985 mm clear aperture whose aims are high resolution imaging and spectral observations, including measurements of the solar magnetic field. It now consists of one channel for the chromosphere and

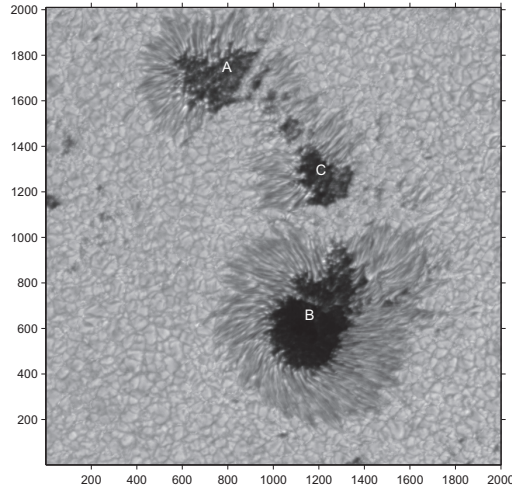


Figure 1. A corrected image of NOAA 12158, whose original image was recorded at 03:00:00 UT on 2014, September 13 with the NVST. The active region included three sunspots marked with the symbol A, B and C.

two channels for the photosphere. The band used for observing the chromosphere is $H\alpha$ (656.3 ± 0.025 nm). The bands for observing the photosphere are the TiO (705.8 ± 1 nm) and the G-band (430.0 ± 0.8 nm). The high-resolution data of the NVST are classified into two levels. The level 1 data are processed by frame selection (lucky imaging) (Tubbs, 2004). The level 1+ data are reconstructed by speckle masking (Lohmann, Weigelt, and Wirnitzer, 1983) or iterative shift and add (Zhou and Li, 1998). Technical details of the NVST were described by Liu *et al.* (2014) and Xu *et al.* (2014).

Because the TiO line is high sensitive to umbral temperature variations (Berdyugina, Solanki, and Frutiger, 2003), the observations of the band are more appropriate to investigating UDs. Therefore, we used the level 1+ TiO observations, rather than the $H\alpha$ and G-band ones. We selected the high-resolution images of six sunspots based on the best seeing conditions since 2012 October. They were obtained from four active regions: NOAA 11598, 11801, 12158, and 12178. The observation parameters are listed in Table 1. The high-resolution data were obtained without adaptive optics. In good seeing conditions, without adaptive optics, the resolution of reconstructed images can almost reach high angular resolution near the diffraction limit of the NVST (Liu *et al.*, 2014).

The images in each sequence were co-aligned by a subpixel registration algorithm (Feng *et al.*, 2012; Yang *et al.*, 2015). From Table 1 we can see that the sunspots of NOAA 11598, 11801, 12158 were away from the solar disk center, especially the sunspot located in NOAA 11801. Its heliocentric angle θ was close to 39 degrees (*i.e.*, $\cos(\theta)=0.78$). So we transformed the three image sequences to heliographic coordinate for correcting the projection effects. Figure 1 shows a corrected sample of NOAA 12158 obtained at 03:00:00 UT on 2014, September 13, in which are three sunspots (A, B and C).

Table 1. Parameter of observed sunspots

AR NOAA	Date	Time interval (UT)	Location	Pixel size (")	Cadence(s)
11598	2012-10-29	05:50:13-07:44:36	S11W27	0.041	37
11801	2013-08-01	03:38:35-04:34:55	W31N24	0.041	20
12158	2014-09-13	02:57:30-03:47:14	N20W27	0.052	30
12178	2014-10-03	04:35:00-05:33:03	S01E05	0.052	40

3. Identification and Tracking of UDs

We followed the method (Feng *et al.*, 2015) to identify and track CUDs and PUDs. The method mainly consists of three steps: firstly, the periphery and center boundary inside the umbra is detected based on the morphological reconstruction technique; secondly, the UDs are identified based on the phase congruency technique, finally, the identified UDs are tracked based on a 26-connected neighborhood technique. The phase congruency technique has been used to extract those low-contrast solar features, like coronal loops and umbral flashes (Feng *et al.*, 2014a,b).

Usually, empirical distance thresholds have been used to divided UDs into CUDs and PUDs (Riethmüller *et al.*, 2008; Watanabe, Kitai, and Ichimoto, 2009; Hamedivafa, 2011; Louis *et al.*, 2012). Riethmüller *et al.* (2008) considered an UD as a PUD if the UD's birth position is closer than 400 km to a defined umbra boundary, otherwise as a CUD. Hamedivafa (2011) defined a narrow width near the umbra boundary with an empirical threshold, in which the UDs are considered as PUDs. Louis *et al.* (2012) considered the threshold 0.8" inward from an assigned umbra boundary as PUDs, the others as CUDs.

Because the definition of the periphery and center boundary is crucial to investigating UDs, we briefly introduce the definition and the identification procedure proposed by Feng *et al.* (2015). They defined the periphery and center boundary according to the umbral profile. We drew a three dimension surface of a corrected image obtained from NOAA 11801 and show it in Figure 2. As illustrated with the red dash line of Figure 2, the profile of the umbra can be approximated by a trapezoid whose two sides appear as skew, and the base is relatively flat. Thus, the base of the trapezoid is defined as the center of the umbra, in which the UDs are considered as CUDs. The legs of the trapezoid are defined as the region of PUDs, *i.e.*, both the slopes. For obtaining the periphery and center boundary of each image, the image is first reconstructed by morphological reconstruction technique, and then two thresholds are used to extract the periphery and center. There, the thresholds, 0.3 and 0.6 R_{max} , were used to obtain the regions. R_{max} denotes the maximum intensity of the reconstructed image.

Two examples including the identified UDs, and the periphery and center boundaries are shown in Figure 3. The periphery and center boundaries are marked with yellow and red curves, and the positions of the identified UDs are

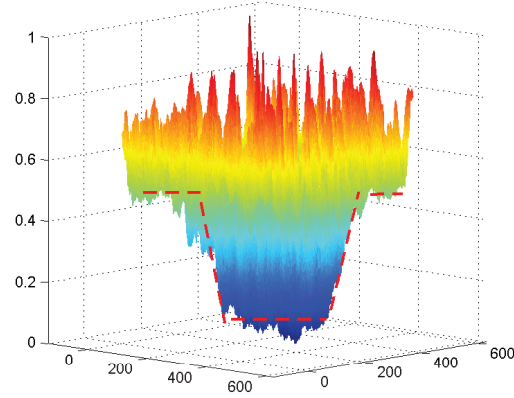


Figure 2. A surface of a corrected sample whose original image was obtained at 03:48:04 UT on 2013, August 1. The red dash line illustrates the umbral profile that can be approximated by a trapezoid.

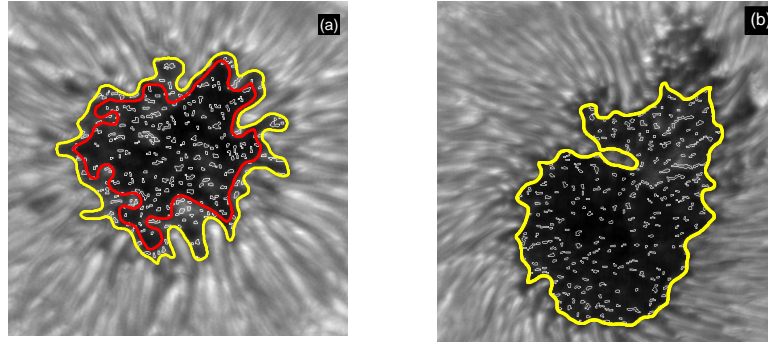


Figure 3. The identified results of UD using the method proposed by Feng *et al.* (2015): (a) the identified result of a corrected sample obtained from NOAA 11801 whose original image was obtained at 03:48:04 UT on 2013, August 1; (b) the identified results of the sunspot marked with symbol B in Figure 1. The umbra-penumbra and periphery-center boundaries are superposed with red and yellow curves, respectively, and the identified UD are marked with white closed curves.

marked with white closed curves. To the three sunspots of NOAA 12158, we only extracted CUDs without PUDs. Therefore, we extracted CUDs from six sunspots and PUDs from three sunspots.

4. Results and Discussion

Firstly, the statistical properties of UD such as equivalent diameter, ratio of the maximum intensity of UD to the mean intensity of the corresponding adjacent umbral background, horizontal velocity, and lifetime were obtained. Secondly, the intensity-diameter, lifetime-diameter, lifetime-intensity, and velocity-

Table 2. The number of the identified UD of each sunspot

AR NOAA	11598	11801	12158			12178
Spot			A	B	C	
CUD	313	201	90	279	75	262
PUD	219	162	0	0	0	222

intensity relationships were analyzed. Finally, the relationships between the properties and the influence under different magnetic fields were discussed.

4.1. Property Definition and Feature Extraction

The property definitions are as follow. For each UD, its equivalent diameter (D_{eq}) is calculated with $\sqrt{4A/\pi}$, where A denotes the total number of pixels of an UD. The coordinate (x_c, y_c) of the centroid and the ratio of the maximum intensity (I_{ud}) to the mean intensity of the adjacent umbral background (I_{bg}) are determined according to the identified areas. The properties are also defined with the tracking procedure: lifetime (T_{ud}), birth-death distance (L_{bd}), and horizontal velocity (V_{ud}). To an UD, T_{ud} is the sum of the cadence of all frames. L_{bd} is the centroid distance from its birth frame to death frame. Horizontal velocity V_{ud} is the ratio of L_{bd} to T_{ud} .

We rejected the UDs whose diameter is lower than 130 km (0.18") and lifetime is less than 2 min for accurate statistical results. In the tracking procedure, if splitting or merging occurred, the UD have to be discarded. Finally, a total of 1220 CUDs and 603 PUDs were obtained. Table 2 lists the number of the CUDs and PUDs of each sunspot. In the following we utilize the UDs to analyze their physical properties and the relationships among the different properties and magnetic field.

4.2. Statistical Properties of UDs

Figure 4 shows the statistical properties and corresponding fitted curves of the CUDs and the PUDs located only in AR NOAA 12178; the others are not shown due to the similar distributions and fit curves. However, all the statistical results are listed in Table 3. The red color indicates the statistics of the CUDs, and the blue color indicates that of the PUDs in Figure 4. Their corresponding fit functions are indicated with the corresponding color curves.

Figure 4a shows the histograms of the equivalent diameters, and their distribution functions. The histograms are fitted using Gaussian functions. The diameter of CUDs ranges from 179 to 235 km, and that of PUDs from 195 to 226 km. The results are in a good agreement with the reports (Hamedivafa, 2008; Riethmüller *et al.*, 2008; Bharti, Beeck, and Schüssler, 2010; Kilcik *et al.*, 2012). These authors found that the diameter range of UDs is between 150 and 350 km.

Table 3. The statistical values of the CUD and PUD properties

CUDs					
NOAA	Spot	Diameter(km)	I_{ud}/I_{bg}	Lifetime(min)	Velocity(km s ⁻¹)
11598		178±40	1.05±0.02	5.35	0.37±0.19
11801		216±38	1.07±0.03	4.48	0.30±0.16
12158	A	235±41	1.10±0.05	5.67	0.27±0.14
12158	B	225±40	1.08±0.04	5.66	0.38±0.20
12158	C	234±45	1.09±0.04	7.26	0.19±0.10
12178		210±38	1.07±0.03	4.59	0.37±0.19
PUDs					
11598		195±41	1.08±0.06	6.25	0.47±0.24
11801		226±46	1.15±0.09	7.95	0.45±0.24
12178		226±41	1.12±8.12	4.59	0.51±0.27

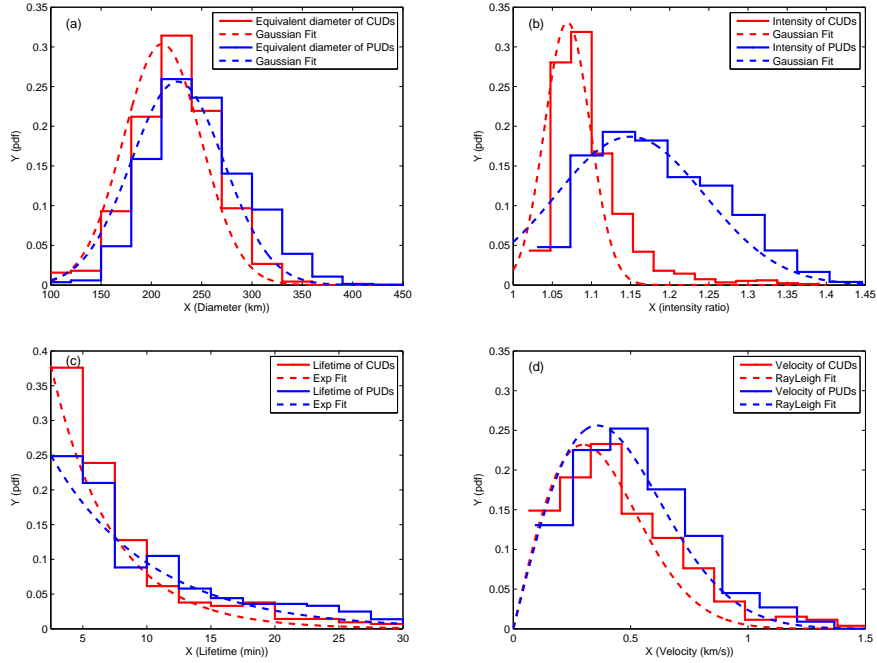
**Figure 4.** The histograms and the distribution curves of the CUDs and PUDs located in the sunspot of NOAA 12178. (a) Equivalent diameter; (b) intensity ratio; (c) lifetime; (d) horizontal velocity. The red color indicates the statistics of the CUDs, and the blue color indicates that of the PUDs.

Figure 4b shows the histogram of the ratio (I_{ud}/I_{bg}), and its fitted distribution. Meanwhile, Gaussian functions are used to fit the distributions. From Table 3 we can see that the intensity ratio of CUDs ranges from 1.05 to 1.10 and PUDs from 1.08 to 1.15. This implies that the brightness of CUDs is higher 5–10 % than their adjacent background, and that of PUDs is 8–15 %.

As shown in Figure 4c, the histograms of the CUDs and PUDs lifetimes appear to be an exponential distribution, so we used exponential functions to fit the distributions. The variation range of the UD lifetimes is between 4 and 7 min. The exponential distribution is in qualitative agreement with the literature (Sobotka *et al.*, 1999; Riethmüller *et al.*, 2008; Hamedivafa, 2011; Feng *et al.*, 2015).

Because the horizontal velocities of the UDs, regardless of CUDs and PUDs, at the X and Y direction exhibit Gaussian distributions, we used Rayleigh functions to fit the velocity distributions. The velocity range of CUDs is between 0.19 and 0.38 km s⁻¹ and that of PUDs ranges from 0.47 to 0.51 km s⁻¹ (see Table 3). The velocity of CUDs and PUDs is also remarkably different, and the horizontal velocity of CUDs is slower than that of PUDs. Our findings are in agreement with the reports (Watanabe, Kitai, and Ichimoto, 2009; Kilcik *et al.*, 2012). These authors concluded the reason that PUDs hold a relatively fast horizontal velocity is that the PUDs locates in a strong horizontal component of the magnetic field and/or strongly inclined fields.

4.3. Correlation Analysis of UDs Properties

The relationships of all CUDs (1220) obtained from six sunspots and all PUDs (603) from three sunspots such as intensity-diameter, lifetime-diameter, lifetime-intensity, and velocity-intensity relationships are presented in the form of scatter plots in Figure 5. There, the green lines are the standard errors of each bin, and the solid red lines are the fitted line based on the bins. Here, the data were divided into 15 groups according to the minimum and maximum values along X axis, and each group is a bin. Note that the division method can cause very little or no data in a bin. As shown in Figure 5d, only five bins are shown although 15 groups were divided. The corresponding correlation coefficients are listed in Table 4. As shown in the left column of Figure 5, we can find that intensity-diameter (5a), lifetime-diameter (5c), and lifetime-intensity (5e) exhibit an increasing trend; however, velocity-intensity (5g) is a decreasing trend. The results indicate that larger CUDs tend to be brighter, live longer and move slower. Although the PUDs trend can also be found (see the right column of Figure 5), we are not very sure about it, because only three spots are included in the sample.

Bharti, Beeck, and Schüssler (2010) concluded from realistic radiative MHD simulations that the area-lifetime and the brightness-lifetime are positively correlated. They stated that the correlations exist due to the fact that stronger and more extended convective upflows are maintained longer and create larger and brighter UDs. Similar trends were found by Tritschler and Schmidt (2002); Sobotka and Puschmann (2009); Kilcik *et al.* (2012). Kilcik *et al.* (2012) studied UDs statistical properties using the observations of the high-resolution data recorded by the New Solar Telescope at the Big Bear Solar Observatory and

Table 4. The correlation coefficients of the CUDs and PUDs

	Intensity-Diameter	Lifetime-Diameter	Lifetime-Intensity	Velocity-Intensity
CUD	0.62	0.38	0.33	-0.19
PUD	0.55	0.47	0.48	-0.19

three-dimensional MHD simulations of sunspots. They drew a conclusion that the velocities of UD are inversely related to their lifetimes. Our finding about the CUDs trends also support the reports above.

4.4. Relationship Between UD Property and Umbral Magnetic Field

In order to analyze the influence to UD properties with respect to different magnetic field, we obtained the radial component of the magnetic field, B_r , of the six sunspots from the *Helioseismic and Magnetic Imager* onboard the *Solar Dynamics Observatory* (SDO / HMI, Schou *et al.*, 2012). Because the pixel scale of HMI image is 0.5'' and UD diameters approximate 0.3'' (Schüssler and Vögler, 2006; Kilcik *et al.*, 2012; Feng *et al.*, 2015; Yan *et al.*, 2015), we fail to obtain the accurate pixel-by-pixel magnetic field features of each UD. Therefore, we used the mean magnetic flux of the periphery and the center of each umbra to analyze the influence. In order to improve the sensitivity of the mean flux density, the B_r maps were selected during the observed time interval to each data set and then averaged. The B_r maps of two sunspots are shown in Figure 6, in which the maps were extended to the same scale with a nearest-neighbor interpolation method and aligned to the corresponding corrected TiO image (*i.e.*, the image shown in Figure 3). There, the periphery and center boundaries are superposed on the magnetic map with yellow and red curves, respectively. The mean flux densities of the periphery and the center according to the corresponding extended magnetic images are listed Table 5. Note that the influence calculating the mean strengths is slight with the interpolated magnetic images. The relationship plots between magnetic flux density and CUD properties (diameter, intensity, lifetime, and velocity) are shown in Figure 7. The green lines are the standard errors of each CUD data sets, and the red dash lines are the fitted ones based on the six sunspots. Their correlation coefficients are -0.87, -0.91, -0.47 and 0.79. The PUD relationship is not shown due to only three data sets. From the fitted lines of Figure 7 we can find that the diameters and the brightness of CUDs have decreasing trend with the magnetic flux density increasing (see Figures 7a and b), and the velocity increases with density increasing (see Figure 7d). However, the lifetimes of CUDs fail to exhibit an obvious trend under different magnetic flux density (see Figure 7c). The results also imply that the CUD is larger and brighter and its motion is slower in a reduced magnetic flux density, however, its lifetime is unrelated to that.

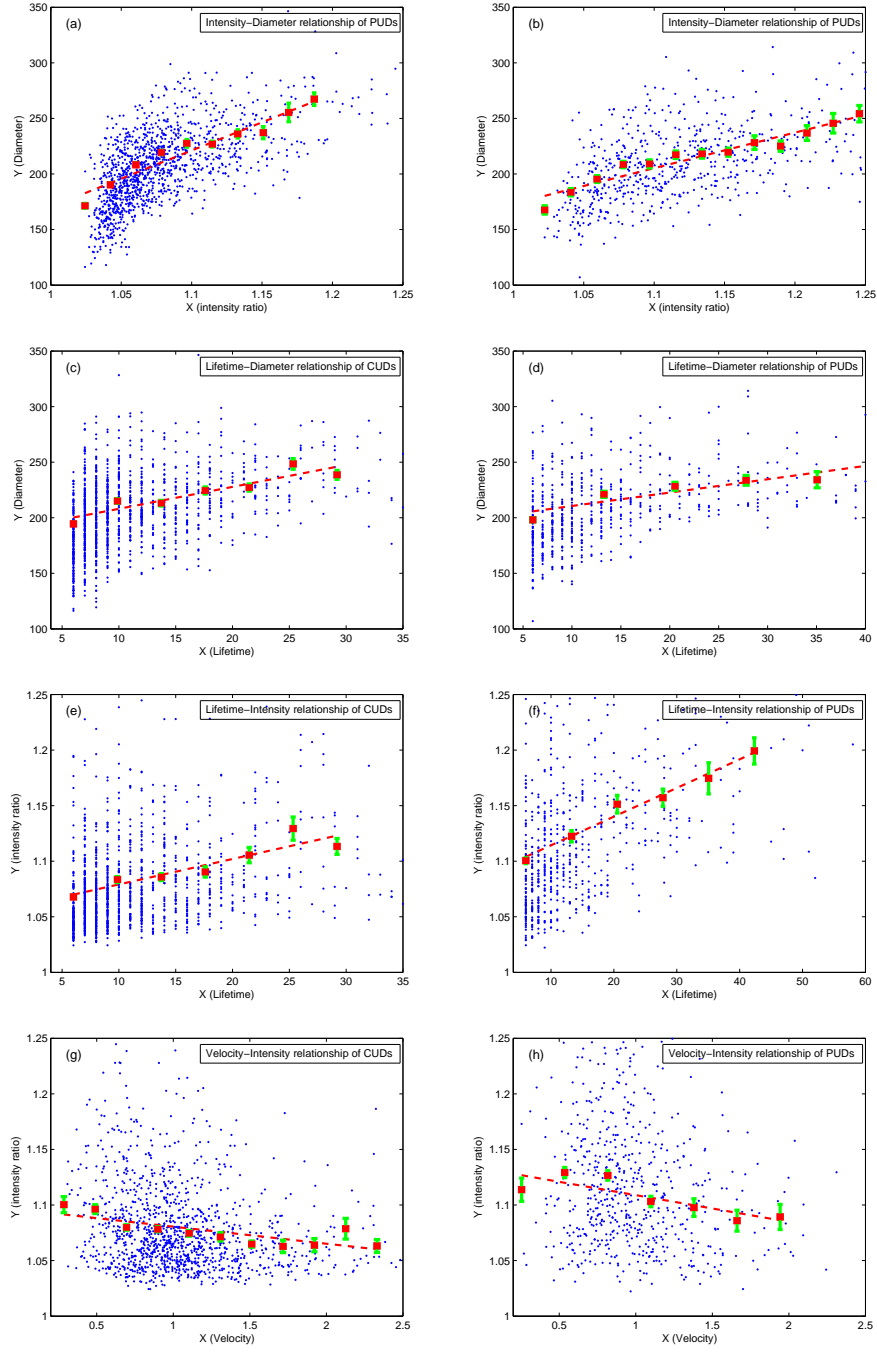


Figure 5. The scatter plots of all CUDs and all PUDs obtained from the four active regions. The left column illustrates the relationships of the CUDs, and the right column illustrates that of PUDs: (a-b) intensity-diameter; (c-d) lifetime-diameter; (e-f) lifetime-intensity; (g-h) velocity-intensity.

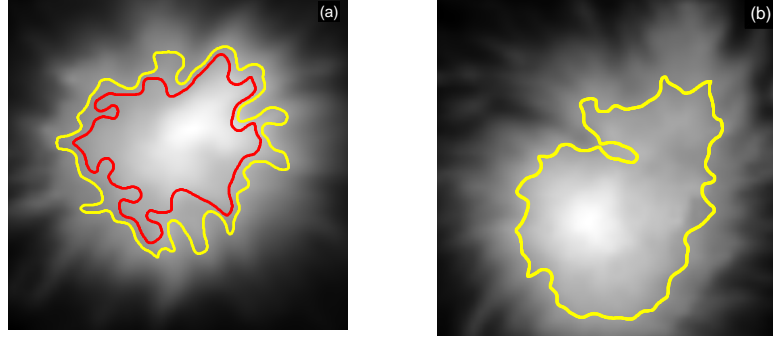


Figure 6. The radial component of the magnetic field B_r superposed on the umbra-penumbra and periphery-center boundaries with red and yellow curves: (a) the B_r map of NOAA 11801 obtained with the SDO / HMI at 03:48:00 UT on 2013, August 1; (b) the B_r map of NOAA 12158 obtained at 03:00:00 UT on 2014, September 13.

Table 5. The mean magnetic flux density of each umbra

CUDs						
AR NOAA	11598	11801	12158			12178
Spot			A	B	C	
Mean Flux Density	2334	2009	1566	2079	1741	2212
PUDs						
Mean Flux Density	1888	1582				1688

5. Conclusion

We selected the high-resolution TiO image sequences of four ARs obtained under the best seeing conditions with the NVST to investigate UD properties and analyze the relationships among different properties. The four ARs include six sunspots, and 1220 CUDs and 603 PUDs were obtained from six and three sunspots, respectively. Subsequently, the magnetic field influence to UD properties was analyzed using the radial component of the magnetic field obtained from the SDO / HMI.

To an UD, regardless of CUDs and PUDs, its diameter and lifetime hold an increasing trend with brightness, whereas its horizontal velocity exhibits an inverse trend. Its diameter becomes larger, and its brightness higher, and its velocity slower in a weak magnetic field than in a strong field. However, the lifetimes of UDs located in different sunspots are not obviously different, implying that the UD lifetime is unrelated to magnetic flux density located.

Note that the trends of PUDs were obtained using the samples of three sunspots. Because CUDs and PUDs have different origins, formation height in the atmosphere, and dynamics, they represent different physical characteristics.

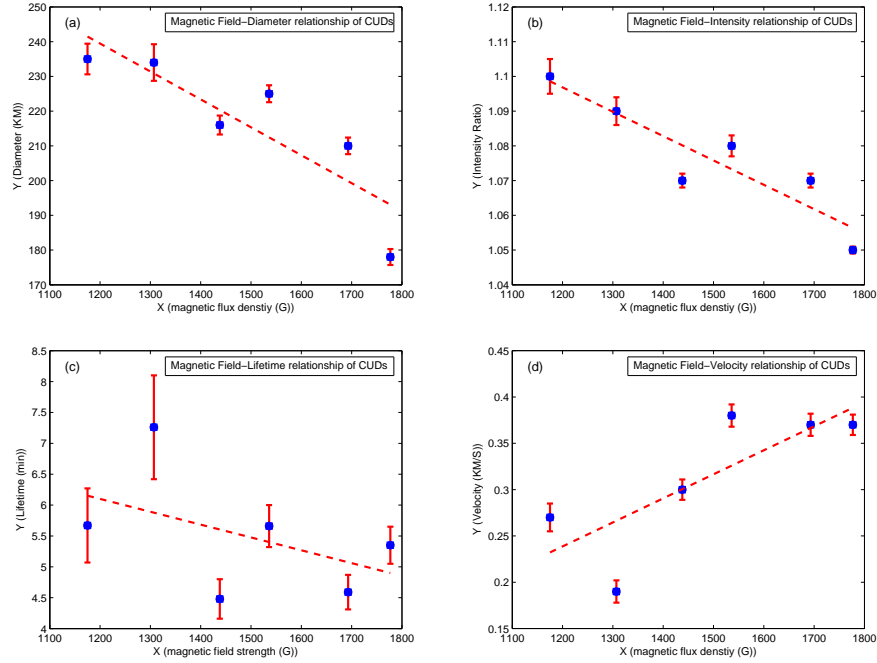


Figure 7. The relationship plots between magnetic flux density and the CUD properties: (a) diameter-magnetic flux density; (b) intensity-magnetic flux density; (c) lifetime-magnetic flux density; (d) velocity-magnetic flux density.

The method divided UDs into CUDs and PUDs based on the umbral profile could mix up both CUDs and PUDs, and distort the statistical results.

Acknowledgements The authors are grateful to the referee for enlightening comments and suggestions that improved the quality of our work. This work is supported by the National Natural Science Foundation of China (Nos: U1231205, U1531132, 11573012, 11463003, 11303011, 11263004, 11163004) and the Open Research Program of Key Laboratory of Solar Activity of Chinese Academy of Sciences (No: KLSA201414, KLSA201505). This work is also supported by the Opening Project of Key Laboratory of Astronomical Optics & Technology, Nanjing Institute of Astronomical Optics & Technology, Chinese Academy of Sciences (No: CAS-KLAOT-KF201306). The authors thank the NVST team for their high-resolution observations.

References

- Berdugina, S.V., Solanki, S.K., Frutiger, C.: 2003, The molecular Zeeman effect and diagnostics of solar and stellar magnetic fields. II. Synthetic Stokes profiles in the Zeeman regime. *Astron. Astrophys.* **412**, 513–527. doi:10.1051/0004-6361:20031473.
- Bharti, L., Beeck, B., Schüssler, M.: 2010, Properties of simulated sunspot umbral dots. *Astron. Astrophys.* **510**, A12. doi:10.1051/0004-6361/200913328.
- Bharti, L., Joshi, C., Jaaffrey, S.N.A.: 2007, Observations of Dark Lanes in Umbral Fine Structure from the Hinode Solar Optical Telescope: Evidence for Magnetoconvection. *Astrophys. J. Lett.* **669**, L57–L60. doi:10.1086/523352.

- Feng, S., Xu, Z., Wang, F., Deng, H., Yang, Y., Ji, K.: 2014a, Automated Detection of Low-Contrast Solar Features Using the Phase-Congruency Algorithm. *Solar Phys.* **289**, 3985–3994. doi:10.1007/s11207-014-0538-2.
- Feng, S., Yu, L., Yang, Y.-F., Ji, K.-F.: 2014b, Identification of emission sources of umbral flashes using phase congruency. *Research in Astronomy and Astrophysics* **14**, 1001–1010. doi:10.1088/1674-4527/14/8/010.
- Feng, S., Zhao, Y., Yang, Y., Ji, K., Deng, H., Wang, F.: 2015, Identifying and Tracking of Peripheral and Central Umbral Dots. *Solar Phys.* **290**, 1119–1133. doi:10.1007/s11207-015-0670-7.
- Feng, S., Deng, L., Shu, G., Wang, F., Deng, H., Ji, K.: 2012, A subpixel registration algorithm for low psnr images. In: *Advanced Computational Intelligence (ICACI), 2012 IEEE Fifth International Conference on*, 626–630. IEEE.
- Grossmann-Doerth, U., Schmidt, W., Schroeter, E.H.: 1986, Size and temperature of umbral dots. *Astron. Astrophys.* **156**, 347–353.
- Hamedivafa, H.: 2008, Application of an Improved Method of Image Segmentation and Some Considerations on Identification and Tracking of Umbral Dots. *Solar Phys.* **250**, 17–29. doi:10.1007/s11207-008-9201-0.
- Hamedivafa, H.: 2011, Kinematics of Umbral Dots: Their Typical Area, Brightness and Lifetime. *Solar Phys.* **270**, 75–88. doi:10.1007/s11207-011-9729-2.
- Kilcik, A., Yurchyshyn, V.B., Rempel, M., Abramenko, V., Kitai, R., Goode, P.R., Cao, W., Watanabe, H.: 2012, Properties of Umbral Dots as Measured from the New Solar Telescope Data and MHD Simulations. *Astrophys. J.* **745**, 163. doi:10.1088/0004-637X/745/2/163.
- Liu, Z., Xu, J., Gu, B.-Z., Wang, S., You, J.-Q., Shen, L.-X., Lu, R.-W., Jin, Z.-Y., Chen, L.-F., Lou, K., Li, Z., Liu, G.-Q., Xu, Z., Rao, C.-H., Hu, Q.-Q., Li, R.-F., Fu, H.-W., Wang, F., Bao, M.-X., Wu, M.-C., Zhang, B.-R.: 2014, New vacuum solar telescope and observations with high resolution. *Research in Astronomy and Astrophysics* **14**, 705–718. doi:10.1088/1674-4527/14/6/009.
- Lohmann, A.W., Weigelt, G., Wirtzner, B.: 1983, Speckle masking in astronomy - Triple correlation theory and applications. *Applied Optics* **22**, 4028–4037. doi:10.1364/AO.22.004028.
- Louis, R.E., Mathew, S.K., Bellot Rubio, L.R., Ichimoto, K., Ravindra, B., Raja Bayanna, A.: 2012, Properties of Umbral Dots from Stray Light Corrected Hinode Filtergrams. *Astrophys. J.* **752**, 109. doi:10.1088/0004-637X/752/2/109.
- Parker, E.N.: 1979, Sunspots and the physics of magnetic flux tubes. IX - Umbral dots and longitudinal overstability. *Astrophys. J.* **234**, 333–347. doi:10.1086/157501.
- Riethmüller, T.L., Solanki, S.K., Zakharov, V., Gandorfer, A.: 2008, Brightness, distribution, and evolution of sunspot umbral dots. *Astron. Astrophys.* **492**, 233–243. doi:10.1051/0004-6361:200810701.
- Schou, J., Scherrer, P.H., Bush, R.I., Wachter, R., Couvidat, S., Rabello-Soares, M.C., Bogart, R.S., Hoeksema, J.T., Liu, Y., Duvall, T.L., Akin, D.J., Allard, B.A., Miles, J.W., Rairden, R., Shine, R.A., Tarbell, T.D., Title, A.M., Wolfson, C.J., Elmore, D.F., Norton, A.A., Tomczyk, S.: 2012, Design and Ground Calibration of the Helioseismic and Magnetic Imager (HMI) Instrument on the Solar Dynamics Observatory (SDO). *Solar Phys.* **275**, 229–259. doi:10.1007/s11207-011-9842-2.
- Schüssler, M., Vögler, A.: 2006, Magnetoconvection in a Sunspot Umbra. *Astrophys. J. Lett.* **641**, L73–L76. doi:10.1086/503772.
- Sobotka, M., Puschmann, K.G.: 2009, Morphology and evolution of umbral dots and their substructures. *Astron. Astrophys.* **504**, 575–581. doi:10.1051/0004-6361/200912365.
- Sobotka, M., Bonet, J.A., Vazquez, M.: 1993, A High-Resolution Study of Inhomogeneities in Sunspot Umbrae. *Astrophys. J.* **415**, 832. doi:10.1086/173205.
- Sobotka, M., Brandt, P.N., Simon, G.W.: 1997a, Fine structure in sunspots. I. Sizes and lifetimes of umbral dots. *Astron. Astrophys.* **328**, 682–688.
- Sobotka, M., Brandt, P.N., Simon, G.W.: 1997b, Fine structure in sunspots. II. Intensity variations and proper motions of umbral dots. *Astron. Astrophys.* **328**, 689–694.
- Sobotka, M., Vázquez, M., Bonet, J.A., Hanslmeier, A., Hirzberger, J.: 1999, Temporal Evolution of Fine Structures in and around Solar Pores. *Astrophys. J.* **511**, 436–450. doi:10.1086/306671.
- Tritschler, A., Schmidt, W.: 2002, Sunspot photometry with phase diversity. II. Fine-structure characteristics. *Astron. Astrophys.* **388**, 1048–1061. doi:10.1051/0004-6361:20020542.
- Tubbs, R.N.: 2004, Lucky exposures: diffraction-limited astronomical imaging through the atmosphere. *The Observatory* **124**, 159–160.

- Watanabe, H., Kitai, R., Ichimoto, K.: 2009, Characteristic Dependence of Umbral Dots on Their Magnetic Structure. *Astrophys. J.* **702**, 1048–1057. doi:10.1088/0004-637X/702/2/1048.
- Watanabe, H., Bellot Rubio, L.R., de la Cruz Rodríguez, J., Rouppe van der Voort, L.: 2012, Temporal Evolution of Velocity and Magnetic Field in and around Umbral Dots. *Astrophys. J.* **757**, 49. doi:10.1088/0004-637X/757/1/49.
- Xu, Z., Jin, Z.Y., Xu, F.Y., Liu, Z.: 2014, Primary observations of solar filaments using the multi-channel imaging system of the New Vacuum Solar Telescope. In: Schmieder, B., Malherbe, J.-M., Wu, S.T. (eds.) *IAU Symposium, IAU Symposium* **300**, 117–120. doi:10.1017/S1743921313010831.
- Yan, X.L., Xue, Z.K., Pan, G.M., Wang, J.C., Xiang, Y.Y., Kong, D.F., Yang, L.H.: 2015, The Formation and Magnetic Structures of Active-region Filaments Observed by NVST, SDO, and Hinode. *The Astrophysical Journal Supplement Series* **219**, 17. doi:10.1088/0067-0049/219/2/17.
- Yang, Y.-F., Qu, H.-X., Ji, K.-F., Feng, S., Deng, H., Lin, J.-B., Wang, F.: 2015, Characterizing motion types of G-band bright points in the quiet Sun. *Research in Astronomy and Astrophysics* **15**, 569. doi:10.1088/1674-4527/15/4/009.
- Zhou, L., Li, C.-S. (eds.): 1998, *Electronic Imaging and Multimedia Systems II, Society of Photo-Optical Instrumentation Engineers (SPIE) Conference Series* **3561**.